Faraday Discussions
Cite this: *Faraday Discuss.*, 2026, **263**, 182

PAPER

Structural purification of technical lignins *via* fractional dissolution using non-azeotropic solvent mixtures†

Reza Ebrahimi Majdar, [a] Federica Ferruti, [b] Marco Orlandi, [bc] Claudia Crestini [de] and Heiko Lange *[bcef]

Received 8th May 2025, Accepted 21st July 2025
DOI: 10.1039/d5fd00075k

Two technical lignins, a softwood kraft lignin (**SKL**) and a wheat straw organosolv lignin (**WSOSL**) were fractionated using a Soxhlet extractor that was connected to a piston pump for solvent movement such that Soxhlet extraction using non-azeotropic solvent mixtures was feasible. Fractionation of the lignins using such solvent mixtures that could be tuned in terms of hydrogen-bond acceptor and donor characteristics and polarities yielded novel fractions not accessible in standard Soxhlet-based fractionations. Two **SKL** fractions could be obtained applying aqueous acetone that displayed homogeneous structural characteristics while differing significantly in molecular weights. **WSOSL** could be gradually purified, allowing for the generation of a rather pure lignin carbohydrate complex (**LCC**) fraction and a purified high molecular weight lignin fraction.

1 Introduction

Biomass, a renewable resource of undisputable importance for the green transition, provides only two classes of aromatic oligomers or polymers, *i.e.*, lignins and tannins. Among these, lignin is most abundant, accounting for around 20–25% of the structural polymers found in land-based lignocellulosic biomass.[1–4] For any type of exploitation of this natural aromatic polymer the available resources are its

[a]*University of Rome 'Tor Vergata', Department of Chemical Science and Technologies, Via della Ricerca Scientifica, 1, 00133 Rome, Italy. E-mail: heiko.lange@unimib.it*
[b]*University of Milano-Bicocca, Department of Earth and Environmental Sciences, Piazza della Scienza, 1, 20126 Milan, Italy*
[c]*NBFC – National Biodiversity Future Center, 90133 Palermo, Italy*
[d]*'Ca' Foscari' University of Venice, Department of Molecular Sciences and Nanosystems, Via Torino 155, 30170 Venice Mestre, Italy*
[e]*NAST – Nanoscience & Nanotechnology & Innovative Instrumentation Center, Via della Ricerca Scientifica, 00133 Rome, Italy*
[f]*Luleå University of Technology, Biochemical Process Engineering, Department of Civil, Environmental and Natural Resources Engineering, Division of Chemical Engineering, 971 87 Luleå, Sweden*
† Electronic supplementary information (ESI) available. See DOI: https://doi.org/10.1039/d5fd00075k

technical derivatives, *i.e.*, the lignins that have been separated from cellulose and hemicellulose in biomass fractionation efforts located in the various biorefinery concepts.[5,6] Isolated technical lignins do resemble the putative natural structure of lignin only more or less, due to the fact that the various physical forces and/or chemistries applied during the biomass fractionation leave structural characteristics and/or impurities in the isolated powders representing the technical lignins.[2,7–9] The structural variety, as well as the impurities contained, represent, however, a notable burden to lignin valorisation in high or higher value applications, and eventually disturb its compatibility with downstream processing.[10] In terms of chemical impurities, residual sugars, present in the form of cellulose fragments, in the degraded form of humins,[11–13] or in the form of covalently bound lignin-carbohydrate complexes (**LCCs**),[14–16] or silicates[17] and other inorganic salts represent the most important examples.

Tailoring lignins to render them more suitable for specific applications often aims at modifying molecular weight characteristics, unifying functional group contents, or purifying them by washing out low molecular weight extractives.[2,8,9] The first aim can be approached by lignin degradation methods, using chemical and biotechnological approaches,[18–21] or by lignin fractionation.[22–26] The second aim is realised either by chemically modifying existing functional groups in lignin or by adding, in abundance, functional motifs by exploiting, in more or less selective ways, reactive groups present in the technical lignins. Washing of lignins, being a less frequently used technique, uses standard extraction methods.

When it comes to the post-isolation fractionation of technical lignins, it is possible to target several of the aforementioned problems of technical lignins, focusing especially on lignin-inherent functional groups and/or molecular weight characteristics. For this aim, chemical, physical, and/or physico-chemical means have been developed. Since the first scientific reports on this field eight decades ago,[27,28] this approach for post-isolation modification of technical lignins has seen various developments. Some more recent reviews highlight achievements and present limitations.[29,30] Commonly used techniques for lignin fractionation comprise sequential/fractional precipitations using either organic solvent systems[31,32] or pH variations in aqueous phases,[33] extractions using single solvents[34,35] or sequential applications of various solvents in fractional dissolution approaches,[36–39] also in continuous processing,[40] and ultrafiltration[41,42] While numerous studies on lignin fractionation do exist by now, only a few of them present also the sufficient amounts of structural data on each fraction that is needed for more direct comparisons (*vide infra*). Approaches using a mixture of physical and chemical treatments coupling solvent extraction with filtration and adsorption can generate fractions that exhibit more sharply defined or novel characteristics.[43,44]

Any of the aforementioned techniques can be applied to representative technical lignins, *i.e.*, lignins that based on their availability can potentially play an important role in the substitution of fossil-based resources. Softwood kraft lignin (**SKL**) and wheat straw organosolv lignin (**WSOSL**) (Fig. 1) are two examples of such representative technical lignins. While the **SKL** represents abundantly available lignins stemming from large scale industrial processes, the **WSOSL** can be seen as a representative of modern lignins isolated in biorefineries that emerged during the last two decades.

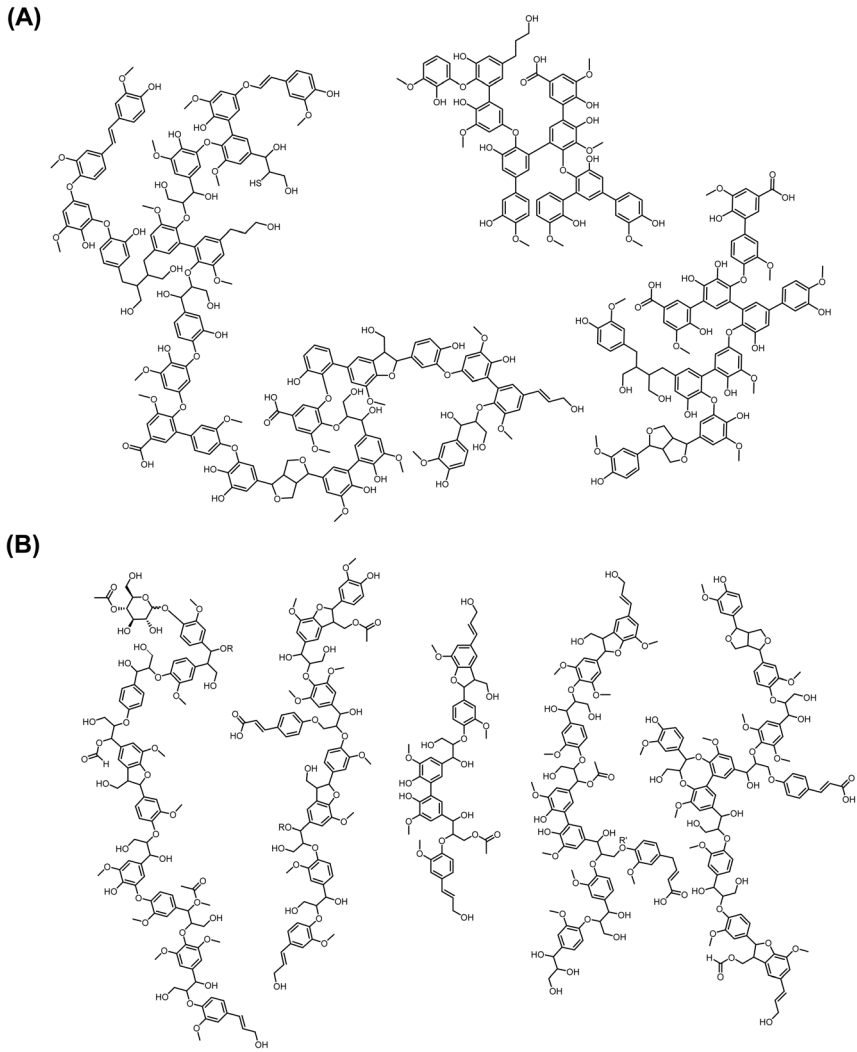

Fig. 1 Structural features of (A) a typical softwood kraft lignin (**SKL**), and (B) a wheat straw organosolv lignin (**WSOSL**).

The softwood kraft lignin (**SKL**) used in the present study was produced *via* the Lignoboost process,[45] and has been subject to numerous studies in our group which allowed for important insights into kraft lignin structure and kraft lignin fractionation.[40,44] On the other hand, a wheat straw-derived organosolv lignin (**WSOSL**) produced *via* the CIMV organosolv biorefinery process,[46] also already investigated in various studies before,[32,39,40,47–51] was used in the current research as a model for modern organosolv lignins. As indicated in the structural representation of **SKL** (Fig. 1A), and demonstrated before, this technical lignin consists of two distinct polymer types, *i.e.*, larger structures showing more 'typical' lignin motifs, and more oligomeric structures that exhibit condensed units caused by the harsh processing conditions. The formylated and acetylated hydroxyl groups in the **WSOSL** (Fig. 1B) are homologous process fingerprints from the CIMV

process.[32] Additionally, as indicated in the structural representation, **LCCs** have been identified before in this **WSOSL**.[39] Both technical lignins were also shown to contain extractives in the form of (degraded) waxes, *etc.*[32,52]

Purification and/or fractionation of the technical lignins, including **SKL** and **WSOSL**, normally exploits Hanson solubility parameters[53] to isolate purified lignins and fractions thereof that differ in both molecular size and functional group content. Especially for purification, but also for fractional dissolution at scale, a Soxhlet-type set-up can be employed, offering a continuous processing upon the refluxing of the solvent or the azeotropic mixture of two or more solvents. When it comes to mixtures of solvents, the necessity of using an azeotrope is limiting, since the azeotrope might not display the necessary solubility parameters. Chromatographic approaches might overcome the limitation of the azeotrope, but introduce eventually a competition between surface interactions of the lignin molecules with the stationary phase and their dissolution in the mobile phase. Flow fractionations might circumvent the need for an azeotrope, but require suitable technical set-ups.

In order to investigate the combined lignin purification/fractionation in a very common and simple set-up such as a Soxhlet filtration without the limitation of the need for azeotropic solvent mixtures, this study employs pump-assisted solvent delivery for a typical Soxhlet set-up. Various non-azeotrope-forming solvent mixtures, or mixtures of solvents that differ from the azeotrope of their binary system, were used to purify and fractionate **SKL** and **WSOSL**. Fractions were analysed by gel permeation chromatography and quantitative ^{31}P NMR spectroscopy, and results were contextualised in light of the insights generated before regarding the two technical lignins.

2 Experimental

2.1 General

Wheat straw organosolv lignin **WSOSL** was produced *via* the Biolignin™ process by CIMV (Compagnie Industrielle de la Matière Végétale), Levallois Perret, France.[46] Softwood kraft lignin, **SKL**, was produced *via* the Lignoboost process[45] by Stora Enso, Kotka, Finland. **WSOSL** and **SKL** were kept at 40 °C in an oven until they reached constant weight. Solvents and reagents in appropriate grades were purchased from Sigma Aldrich and used as received if not stated otherwise.

2.2 Pump-assisted Soxhlet fractionation of SKL and WSOSL

Typically 5 g of a technical lignin, or alternatively of an already derived fraction thereof, were placed in a cellulose thimble inside a Soxhlet extractor. The solvent chosen for the respective extraction step, typically 125 mL, was placed in a two neck round bottom flask connected to the extractor. A Teflon tube (i.d. 1.5 mm) was immersed in the solvent through the second neck and connected to the inlet of a preparative HPLC pump. The outlet of the pump was connected to Teflon tube (i.d. 1.0 mm) that led into the Soxhlet extractor, allowing the stream of solvent arriving at the centre of the surface of the lignin inside the thimble. Liquid–solid extractions were continued until the polydiode array (**PDA**) detector placed in-line after the pump was indicating a constant concentration of UV-active compounds in the solvent, using $\lambda = 280$ nm as the monitoring

wavelength. A refractive index detector was placed in line after the **PDA** detector for eventually monitoring carbohydrate components in the solvent mixtures. Flow rates delivered by the pump were adjusted to have extraction cycles of approx. 15 min. Lignin fractions were isolated by drying the thimble and collecting the contents, and by removing the solvent from the liquid fraction *in vacuo*. Final drying was achieved by placing the samples in a vacuum oven at 40 °C until constant mass was reached.

2.3 ATR-FT-IR analysis

Infrared (IR) spectra were recorded using a Thermo Scientific™ (Thermo Fisher Scientific, Waltham, MA USA) Nicolet™ iS10 FTIR Spectrometer with Attenuated Total Reflectance (ATR) mode. The instrument was equipped with the Thermo Scientific™ Smart iTR™ ATR Sampling Accessory (with a diamond crystal component) and Thermo Scientific™ OMNIC" Spectra Software. All spectra were recorded using an 8 cm^{-1} resolution with 32 scans in the 4000–525 cm^{-1} range, and the total collection time for each sample was 47 seconds. A background collection was performed before every sample analysis.

2.4 ^{31}P NMR analysis

In general, a procedure similar to the one originally published and previously applied was used.[54,55] Approx. 30 mg of the lignin were accurately weighed in a volumetric flask and suspended in 400 μL of a solvent mixture of pyridine and deuterated chloroform ($CDCl_3$) (1.6 : 1 v/v). One hundred microlitres of the internal standard solution, *i.e.*, cholesterol at a concentration of 0.1 M in the aforementioned NMR solvent mixture, were added. 50 mg of Cr(III) acetyl acetonate were added as a relaxation agent to this solution, followed by 100 μL of 2-chloro-4,4,5,5-tetramethyl-1,3,2-dioxaphospholane (Cl-TMDP). After stirring for 120 min at ambient temperature, ^{31}P NMR spectra are recorded on a Bruker 400 MHz NMR spectrometer controlled by TopSpin 2.1 software, with the probe temperature set to 20 °C. The Bruker sequence zgig in qsim acquisition mode was used, with NS = 64; TD = 32 768; SW = 60.0000 ppm; O1 = 42 510.24 Hz; O2 = 3290.40 Hz; $D1$ = 10 s; acquisition time = 963.4586 ms; $P1$ = 6.20 μs. Drift correction and zero-filling were performed prior to Fourier transform. Chemical shifts are expressed in parts per million (ppm) from 85% H_3PO_4 as an external reference; all chemical shifts reported are relative to the reaction product of water with Cl-TMDP, which gives a sharp signal in pyridine/$CDCl_3$ at 132.2 ppm. The maximum standard deviation of the reported data is 0.02 mmol g^{-1}, while the maximum standard error is 0.01 mmol g^{-1}.[54,55] NMR data were processed with MestreNova (Version 8.1.1, Mestrelab Research).

2.5 Gel permeation chromatographic analyses

For gel permeation chromatography (GPC), approx. 2–3 mg of lignin were dissolved in HPLC-grade dimethylsulfoxide (DMSO) (Chromasolv®, Sigma-Aldrich) containing 0.1% (m/v) lithium chloride (LiCl). A Shimadzu instrument was used consisting of a controller unit (CBM-20A), a pumping unit (LC 20AT), a degasser (DGU-20A3), a column oven (CTO-20AC), a diode array detector (SPD-M20A), and a refractive index detector (RID-10A), and controlled by Shimadzu LabSolutions (Version 5.42 SP3). For separation, a PLgel 5 μm MiniMIX-C column (Agilent, 250 × 4.6 mm) was

eluted at 70 °C at 0.25 mL min^{-1} flow rate with HPLC-grade DMSO containing 0.1% lithium chloride for 20 min. Alternatively, three analytical GPC columns (each 7.5 × 30 mm) in series were used: Agilent PLgel 5 μm 10 000 Å, followed by Agilent PLgel 5 μm 1000 Å, followed by an Agilent PLgel 5 μm 500 Å. In this case, HPLC-grade DMSO containing 0.1% (m/v) lithium chloride was used at 0.25 mL min^{-1} for 70 min at 70 °C column temperature. Standard calibration was performed in both column set-ups using polystyrene sulfonate standards in acid form (Sigma Aldrich, MW range 0.43–2.60 × 10^6 g mol^{-1}); lower calibration limits were verified by monomeric and dimeric lignin models. Final analysis of each sample was performed using the intensities of the UV signal at $\lambda = 280$ nm employing a tailor-made MS Excel-based table calculation, in which the number average molecular weight (Mn) and the weight average molecular weight (Mw) are calculated based on the measured absorption (in a.u.) at a given time (min) after corrections for baseline shift and drift as described before.[56] Analyses were run in duplicate.

2.6 Gas chromatographic analyses of extractives of selected fractions

Gas chromatographic-mass spectrometric analyses of the dried extractives were performed by suspending a dried sample of an isolated fraction of extracts in 500 μL of ethyl acetate, shaking it for two minutes, and filtering the suspension through a syringe filter (0.25 μm pore size, PVDF). The chromatographic separations were performed using a Shimadzu GCMS QP2020NX (Shimadzu Corporation, Kyoto, Japan) equipped with Shimadzu autosampler AOC20i. An SH-Rxi-5ms fused silica capillary column (stationary phase (5%-phenyl)-methylpolysiloxane, 30 m × 0.25 mm i.d., 0.25 μm, Shimadzu Corporation, Kyoto, Japan) was used as the stationary phase, and He (UHP grade) as the carrier gas. The system was operated in 'linear velocity mode' with a starting pressure of 100 kPa, 280 °C injection temperature, and 280 °C interface temperature. The injection volume was 2 μL, and the injection port operated in splitless mode. The temperature program was set as follows: the initial temperature of 50 °C was held for 1 min, then increased at a rate of 10 °C min^{-1} to a 280 °C, which was maintained for 15 min. The MS operated in electron ionization mode (EI) at 70 eV, acquiring in full-scan mode spanning from m/z 50–500. LabSolutions-GCMS Version 4.54 software (Shimadzu Corporation) was used for system control, instrument management and data acquisition. Substances were identified using NIST MS Search, version 2.4 (2020).

3 Results and discussion

3.1 SKL fractionation

SKL was chosen as first technical lignin to be fractionated using a 1 : 1 mixture of acetone and water as a binary solvent system that does not form an azeotrope, using the set-up shown in Fig. 2. After the initial solvent delivery in the desired volume ratio, *i.e.*, here 50% acetone in water, the inlet was changed to the port connected to the flask, entering into a looped set-up that recirculated the solvent that enriched in extractable components with time. An in-line **PDA** detector and an in-line refractive index detector were used for monitoring the gradually increasing concentration of UV-active components at a wavelength of $\lambda = 280$ nm for identifying the point when a plateau was reached. At unchanging UV-

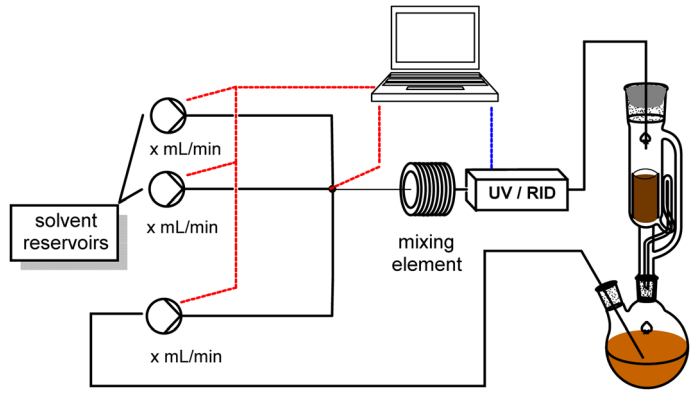

Fig. 2 Scheme of pump-enabled Soxhlet-extractions of technical lignins.

intensities, the flow was stopped and the soluble fraction **AWS-SKL** was isolated alongside the insoluble **AWI-SKL** fraction, in yields of 39% and 60%, respectively. Analysis of the two fractions using gel-permeation chromatography (**GPC**) resulted in the solution profiles shown in Fig. 3A and the estimated molecular weight key parameters listed in Table 1, entries 1–3.

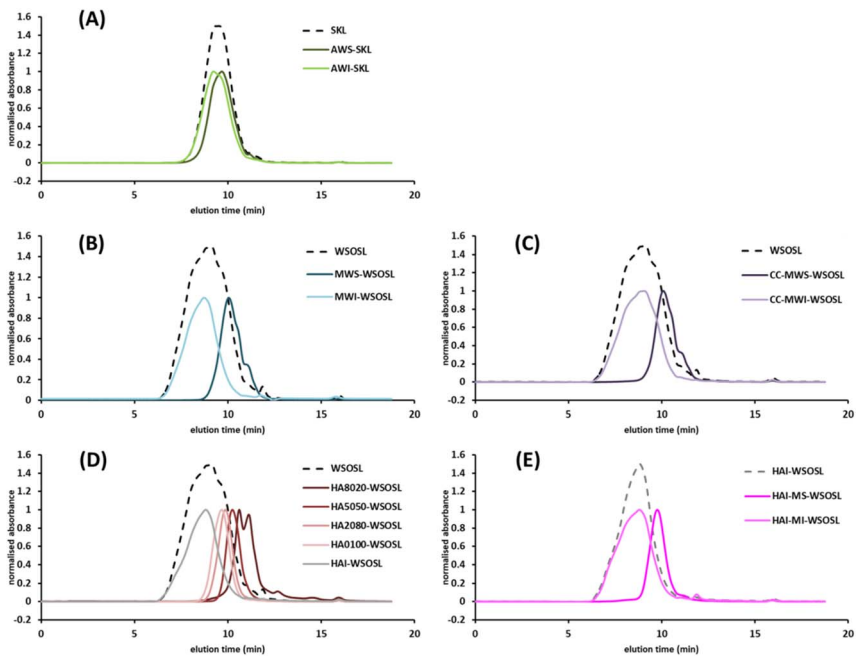

Fig. 3 Traces of GPC-analyses of **SKL** and **WSOSL** and derived fractions thereof: (A) fractionation of **SKL** using acetone–water mixture (50% (v/v)); (B) fractionation of **WSOSL** using methanol–water mixture (50% (v/v)); (C) fractionation of **WSOSL** packed in a column chromatography cartridge using methanol–water mixture (50% (v/v)); (D) fractionation of **WSOSL** using hexane–acetone mixtures of varying compositions (hexane to acetone 80 : 20 (v/v), 50 : 50 (v/v), 20 : 80 (v/v), 0 : 100 (v/v)); and (E) fractionation of hexane–acetone-insoluble **WSOSL** (**HAI-WSOSL**) using methanol.

Table 1 Yields and molecular mass key characteristics of SKL, WSOSL, and derived fractions

Entry	Sample	Yield [%]	Mn [Da]	Mw [Da]	I
1	**SKL**	—	2500	7600	3.0
2	**AWS-SKL**	39	2000	4400	2.1
3	**AWI-SKL**	60	2600	9900	3.9
4	**WSOSL**	—	2100	8600	4.1
5	**MWS-WSOSL**	7.2	1400	5500	3.9
6	**MWI-WSOSL**	93	3200	7200	2.3
7	**CC-MWS-WSOSL**	8.1	1500	5400	3.7
8	**CC-MWI-WSOSL**	92	3100	7100	2.3
9	**HA1000-WSOSL**	<1	n.d.	n.d.	n.d.
10	**HA8020-WSOSL**	1.5	1100	4200	3.8
11	**HA5050-WSOSL**	5.6	1400	2800	2.0
12	**HA2080-WSOSL**	7.5	1700	6500	3.7
13	**HA0100-WSOSL**	8.9	1800	4500	2.3
14	**HAI-WSOSL**[a]	76	2800	11 100	3.9
15	**HAI-MS-WSOSL**	2.3	1900	2600	1.4
16	**HAI-MI-WSOSL**[a]	73	2600	12 000	4.6

[a] Sample not fully soluble, data indicative.

Dimethyl sulfoxide (DMSO) was used as solvent for GPC analyses since it was previously shown to solubilize different lignins and fractions, without the need for the tedious and eventually structure-changing acetobromination.[56,57] In order to prevent aggregation of molecules by excessive electronic interactions between aromatic moieties and hydroxyl–π-interactions, lithium chloride was added to the DMSO used for both sample preparation and chromatographic analyses. In order to verify differences in elution profiles, two different analytical set-ups were used, one employing a single column and one employing the widely used series of three analytical columns. While the use of three columns allowed for a better resolution and more detailed elution profile of each component, the single column set-up was sufficient for evidencing molecular weight differences, as visible in Fig. 3. As seen from the elution traces, and the molecular weights, **AWS-SKL** differs significantly in size from **AWI-SKL**, with the latter exhibiting a molecular weight roughly twice as high as the former.

More interesting are the structural insights obtained by FT-IR spectroscopy and quantitative ^{31}P NMR spectroscopy. Only small characteristic structural differences were highlighted between **AWS-SKL** and **AWI-SKL**, with both fractions displaying the bands typical for **SKL**, as evident from the spectra shown in Fig. 4A.

Hydroxyl groups centred around 3380 cm^{-1} are dominant. C–H stretching vibrations cause characteristic band patterns around 2940, 2880 and 2835 cm^{-1}. Unconjugated C=O carbonyl groups cause a small band around 1720 cm^{-1}. A band at 1690 cm^{-1} indicates enol ethers, while the band at 1590 cm^{-1} and the band pattern around 1510 cm^{-1} are typical for the aromatic backbone. Bands attributable to C–H deformation and the stretching of aromatic rings are found at 1450 and 1425 cm^{-1}, respectively. C–O stretching of the methoxy-groups present in condensed units and G-type aromatics is well reflected by the band identifiable at 1370 cm^{-1}. Alkyl–aryl ethers in the backbone cause bands around 1270 and 1211 cm^{-1} due to the stretching of contained C–O motifs. Within the fingerprint

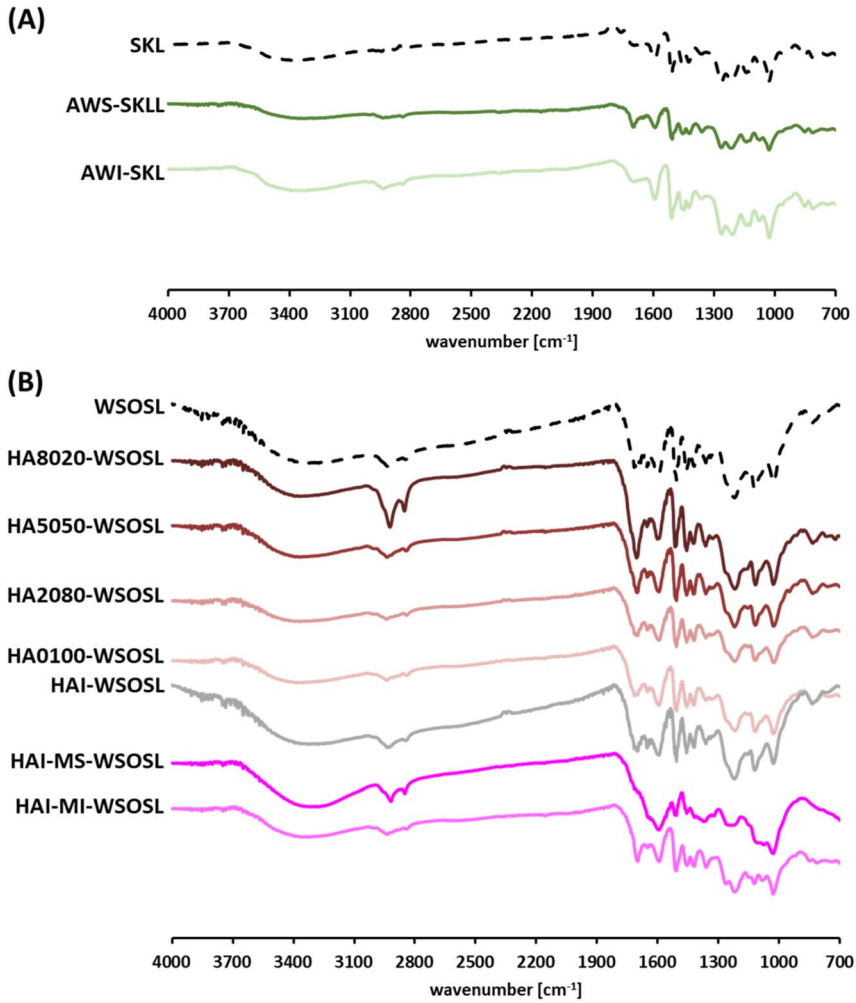

Fig. 4 Overlay of FT-IR spectra obtained for selected fractions in comparison to the starting lignins for (A) SKL and (B) WSOSL.

region, distinct bands representing the C–O stretching of alkyl ethers are found at 1140, 1125, 1080, and 1030 cm^{-1}, respectively. Out of plane vibration modes of C–H bonds are present of 850, 810 and 740 cm^{-1}, respectively.

The structural similarity is confirmed by the qualitative and quantitative analyses of the OH-group contents of the two fractions by ^{31}P NMR spectroscopy (Table 2, entries 2 and 3).

The two fractions do not exhibit the striking structural differences observed when fractionating **SKL** using acetone alone in a Soxhlet set-up,[44] or when using a fractional precipitation with hexane–acetone mixtures.[52] While the acetone is exclusively hydrogen-bond accepting, an acetone–water system should show an equilibrated behavior, with the water being strongly donating and thus contrasting with the donating characteristics that the hydroxyl group in the lignin can exert. In this context, an eventually more abundant hydroxyl group content in a lignin

Table 2 OH-group contents obtained for **SKL**, **WSOSL** and derived fractions determined *via* quantitative ^{31}P NMR after phosphitylation using 2-chloro-4,4,5,5-tetramethyl-1,3,2-dioxaphospholane

Entry	Sample	Aliphatic OH [mmol g^{-1}]	Aromatic OH [mmol g^{-1}]			Acidic OH [mmol g^{-1}]	Arom. OH/aliph. OH
			Condensed	Guaiacyl	*p*-Hydroxy		
1	**SKL**	2.08	1.98	1.89	0.21	0.37	1.96
2	**AWS-SKL**	1.84	1.94	2.15	0.25	0.44	2.36
3	**AWI-SKL**	1.95	1.96	1.81	0.25	0.35	2.07
4	**WSOSL**	1.35	0.42	0.47	0.15	0.31	0.77
5	**MWS-WSOSL**	2.93	0.71	0.80	0.28	0.93	0.61
6	**MWI-WSOSL**	1.43	0.77	0.60	0.28	0.36	1.15
7	**CC-MWS-WSOSL**	2.70	0.91	0.98	0.33	0.98	0.82
8	**CC-MWI-WSOSL**[a]	1.25	0.71	0.49	0.25	0.30	1.16
9	**HA1000-WSOSL**	n.d.	n.d.	n.d.	n.d.	n.d.	n.d.
10	**HA8020-WSOSL**	0.96	0.36	0.51	0.16	1.36	1.08
11	**HA5050-WSOSL**	1.67	1.59	1.88	0.70	1.36	2.49
12	**HA2080-WSOSL**	1.77	1.19	0.99	0.39	0.52	1.46
13	**HA0100-WSOSL**	1.94	1.06	0.75	0.33	0.39	1.10
14	**HAI-WSOSL**[a]	1.57	0.72	0.43	0.24	0.28	0.88
15	**HAI-MS-WSOSL**	3.73	0.47	0.46	0.19	0.84	0.30
16	**HAI-MI-WSOSL**[a]	1.38	0.57	0.42	0.19	0.14	0.86

[a] Sample not fully soluble, data indicative.

molecule becomes less determining in the context of the fractionation. Additionally, the presence of water in the system is interfering significantly with the intermolecular interactions present within a lignin oligomer or polymer. Imagining a more extended lignin molecule, that is interaction with a hydrogen-donating and -accepting solvent can explain the functional group variation observed. The use of a non-azeotropic solvent mixture thus allows for a lignin fractionation exclusively based on molecular weight features, without any significant dissimilarity in the content of hydroxyl groups in the two fractions, thanks to the solvent mixture displaying solubility parameters in terms of hydrogen-bond donating and accepting features that do not favour certain functional groups over others in **SKL**. Apparently, in this case, fractionation is solely based on the capacity of the solvent mixture to solubilise the lignin molecules, *i.e.*, to interact with inter- and intramolecular forces, *i.e.*, various types of hydrogen bonding including hydrogen–π bonding, that cause lignin aggregation and coil formation, with larger molecules exhibiting intramolecular forces that cannot be contrasted by the binary solvent mixture under the applied conditions.[58]

3.2 WSOSL fractionation

WSOSL fractionation was initially performed employing a 1 : 1 mixture (v/v) of methanol and water using the Soxhlet set-up shown in Fig. 2. Using the in-line **PDA** detector for estimating completion of extraction, a soluble **MWS-WSOSL** and an insoluble **MWI-WSOSL** fraction were obtained. The soluble fraction accounted for only around 7% of the lignin used for the experiment. The results

correspond in general to what is commonly observed for this and other organosolv lignins, *i.e.*, a reduced solubility in water-based or water-containing systems unless the pH is adjusted to generate an alkaline milieu. The two fractions differ significantly in molecular weight, with the soluble fraction being roughly in the range of tetramers, whereas GPC suggests the presence of larger oligomers in the insoluble fraction (Table 2, entries 5 and 6). Noticeably, polydispersity is slightly higher for the soluble fraction than for the insoluble one. It is important to note, however, that difficulties were encountered when solubilizing the sample in DMSO for GPC analysis, so that effective molecular weight figures for **MWI-WSOSL** are most probably higher than the ones determined.

Considering FT-IR (data not shown) and ^{31}P NMR analyses (Table 2, entries 5 and 6), fractionation of **WSOSL** with the non-azeotropic mixture exhibiting strong hydrogen-bonding donor capabilities, yielded **MWS-WSOSL** as a lignin enriched in **LCCs** and extractives like waxes, whereas the insoluble **MWI-WSOSL** can be seen as a purified lignin. These results are in line with previous findings, in which an acetone-insoluble-methanol-soluble fraction was identified as an **LCC**-fraction of the **WSOSL** under study.

Since the Soxhlet-based fractionation does not involve a specific packing of the material, and since the contact time of solvent mixture with the lignin to dissolve is long compared to approaches that use chromatographic or continuous dissolution approaches,[25,40] fractionation efficiencies might differ from the mentioned methods. In order to test the effect of a slight back pressure generated by the system and the packaging density of the material, the fractionation with 50% (v/v) aqueous methanol was repeated using a column chromatography cartridge filled with **WSOSL** instead of the Soxhlet extractor. The results obtained for molecular masses and structural features for soluble **CC-MWS-WSOSL** and insoluble **CC-MWI-WSOSL** do not differ significantly from those obtained in the much simpler Soxhlet set-up (Table 2, entries 7 and 8, as well as 5 and 6, respectively.). This observation confirms that within the range of low pressures of up to approx. 3–4 bar (determined *via* the in-built pressure sensor in the pump used for solvent delivery), at ambient temperatures, solubility and fractionation efficiency depend solely on the solvents employed.

For testing the separating capability of non-azeotropic solvent mixtures displaying only hydrogen bond acceptor characteristics and varying polarities, **WSOSL** was fractionated using a common hexane–acetone system in the Soxhlet set-up shown in Fig. 2. Elution profiles of the various soluble fractions obtained from hexane–acetone ratios 80 : 20, 50 : 50, 20 : 80 and 0 : 100 (v/v) are displayed in Fig. 3D. The clear differences between the elution profiles depending on the relative composition of the hexane–acetone mixtures indicate that the Soxhlet set-up under study is capable of delivering fractions with higher resolution, displaying distinct molecular weight features (Table 1, entries 9–12) and structural characteristics (Table 2, entries 9–12). Most interestingly, this fractionation represents not a combined purification/fractionation as observed in case of using the methanol–water mixture that led to the accumulation of both extractives and **LCCs** in one fraction, but in a distinct purification and fractionation. While the hexane-extraction of **WSOSL** delivered **HA1000-WSOSL** in the form of traces of extracts identifiable as alkanes, terpenes and fatty acids (gas-chromatographic analyses, results not shown) and **HA8020-WSOSL** shows the over-proportionally intense signal indicative of fatty acids, purification is achieved when using 20%

(v/v) and 50% (v/v) acetone in hexane. This trend is delineable from the structural data obtained for **HA8020-WSOSL** and **HA5050-WSOSL** (Table 2, entries 9 and 10). The less polar mixture delivers mainly extractives in the form of fatty acids, alkanes, waxes, terpenes, and steroids mixed with lowest molecular weight lignin fragments, as confirmed by FT-IR spectroscopy (Fig. 4B) and by gas-chromatographic analyses (results not shown). The more polar **HA5050-WSOSL** fraction consists already in low molecular weight lignin fragments, not exhibiting any more an over-proportionally intense signal indicative of fatty acids. The difference in quality between the two fractions is clearly visible in the ^{31}P NMR spectra obtained for the two fractions, as shown in Fig. 5.

Upon further increasing the acetone concentration, two more lignin fractions are obtained, in the form of **HA2080-WSOSL** and **HA0100-WSOSL**. The two fractions represent medium molecular weights around 1700–1800 Da, with **HA2080-WSOSL** exhibiting a rather high polydispersity. Both fractions were obtained in rather low yields of 7.5% and 8.9%, respectively. In total, the hexane–acetone extractable fractions account for approx. 22% of the **WSOSL** sample analysed. This observation corresponds to previous findings on this **WSOSL** using a fractional precipitation approach based on hexane–acetone mixtures, in which 80% of the sample remained undissolved in acetone.[32]

The insoluble fraction remaining at this point, *i.e.*, hexane–acetone-insoluble **WSOSL** (**HAI-WSOSL**), displayed poor solubility during the analyses by GPC and ^{31}P NMR, causing an unusually high uncertainty with respect to the values obtained for molecular weight and OH-group content, respectively. Nevertheless, the available data indicate that **HAI-WSOSL** is of larger molecular weight and contains

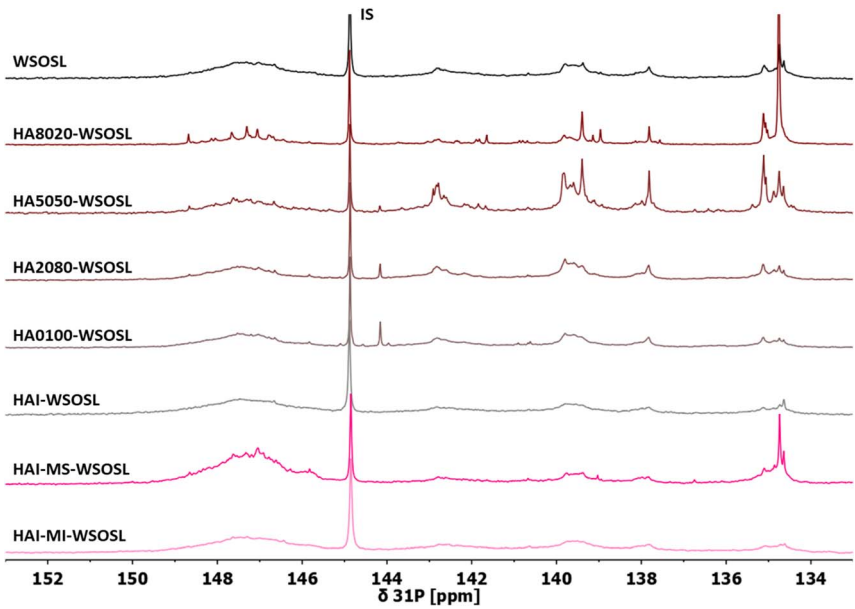

Fig. 5 Comparison of ^{31}P NMR spectra obtained for the fractions obtained upon WSOSL fractionation with various mixtures of hexane–acetone, and the fractionation of the hexane–acetone insoluble fraction using methanol. IS: internal standard cholesterol. Single spectra are shown separately in the ESI.†

significantly more aliphatic hydroxyl groups with respect to aromatic OH-groups when compared to **HA5050-**, **HA2080-**, and **HA0100-WSOSL**. An alternative analysis technique that could eventually further sustain this finding while circumventing the solubility issues is solid state NMR analysis. With respect to qualitative and quantitative OH-group analyses, a derivatization of the OH-groups of the sample, for example *via* esterification, might be beneficial beforehand.[59,60]

In light of the above discussed findings for the fractionation of **WSOSL** using hexane–acetone mixtures and results obtained for **WSOSL** using the methanol–water mixture, **HAI-WSOSL** was subjected to a simple fractionation using pure methanol, to extract the **LCC**-fraction of **WSOSL** that was yet not extracted in the hexane–acetone series. Flowing methanol across the Soxhlet set-up did in fact result in a clear signal increase in both in-line detectors, *i.e.*, the PDA detector and the refractive index detector. Upon steady absorbance levels being detected in the PDA detector, the soluble fraction was isolated as **HAI-MS-WSOSL** in a yield of 2.3%. Spectroscopic analysis *via* ^{31}P NMR (Table 2, entry 14) revealed values similar to those obtained before for the **MWS-WSOSL** and the **CC-MWS-WSOSL** fractions, *i.e.*, a rather high amount of aliphatic OH-groups with respect to aromatic OH-groups. In the case of **HAI-MS-WSOSL**, the ratio of aromatic OH-groups *vs.* aliphatic ones drops to 0.3, strongly indicating the presence of carbohydrates. These values are also in line with data obtained in a previous study[39] for an **LCC**-fraction of the **WSOSL**. Molecular weight data suggest rather oligomeric than polymeric structures (Table 2, entry 14).

The remaining insoluble fraction, *i.e.*, **HAI-MI-WSOSL**, obtained in 76%, can be interpreted, at this point, as a fully purified higher molecular weight wheat straw organosolv lignin, as spectrometric and spectroscopic data corroborate (Table 2, entry 15). As such, this fraction represents a very interesting and very easily accessible starting point for valorisation approaches.

The isolated fractions **HA8020-**, **HA5050-**, **HA2080-**, and **HA0100-WSOSL** were analysed additionally by gas-chromatography coupled to mass spectrometry to determine the nature of the extractives present in the **WSOSL** under study[32] that were carried through the fractionation process. The analyses revealed that the extractives were found especially in the first two fractions, *i.e.*, **HA8020-WSOSL** and **HA5050-WSOSL**, with the former showing the highest amount, Fractions **HA2080-WSOSL** and **HA0100-WSOSL** did not contain significant amounts of extractives. This can be understood by the simple fact that the generation of the first two fractions resembled the typical exhaustive extraction process normally applied for isolating extractives using a Soxhlet extractor.

4 Conclusions

The presented fractionation approach based on simple solvent delivery *via* a piston pump to a Soxhlet extractor allowed for the use of non-azeotropic mixtures of solvents and thus the generation of solubility parameters and H-bonding characteristics that cannot be realised normally in a Soxhlet-based fractionation scenario. The approach delivered novel fractions of two technical lignins, *i.e.*, a softwood kraft lignin (**SKL**) and a wheat straw organosolv lignin (**WSOSL**). In case of the **SKL**, the approach employing aqueous acetone yielded structurally rather homogeneous fractions differing only in molecular weight. Such a result is normally only obtained when using an ultrafiltration

approach working with the black liquor.[41] Fractionating **WSOSL** in the pump-assisted set-up that additionally benefits from optional in-line detection tools such as PDA or refractive index detectors, allowed for the targeted purification and subsequent fractionation of the lignin. A clean **LCC**-fraction could be obtained alongside a **WSOSL** fraction that is of higher molecular weight than the starting material while being free of **LCCs** and extractives, representing as such an ideal starting point for valorisation approaches that might benefit from the use of a lignin that is close to the putative natural form of lignin. The presented procedure is scalable, given the available instruments for larger scale and paralleled Soxhlet extractions.

Abbreviations

AWI-SKL	Acetone-water insoluble softwood kraft lignin
AWS-SKL	Acetone-water soluble softwood kraft lignin
CC	Column chromatography cartridge
DMSO	Dimethyl sulfoxide
FT-IR	Fourier transform infrared
GPC	Gel permeation chromatography
HAXXYY-WSOSL	Hexane–acetone soluble wheat straw organosolv lignin, where XX and YY indicate the relative content of hexane and acetone respectively, in the solvent mixture
HAI-MI-WSOSL	Hexane–acetone insoluble methanol insoluble wheat straw organosolv lignin
HAI-MS-WSOSL	Hexane–acetone insoluble methanol soluble wheat straw organosolv lignin
HAI-WSOSL	Hexane–acetone insoluble wheat straw organosolv lignin
I	Polydispersity index
LCC	Lignin carbohydrate complex
Mn	Number average molecular weight
MW	Molecular weight
Mw	Weight average molecular weight
MWI-WSOSL	Methanol–water insoluble wheat straw organosolv lignin
MWS-WSOSL	Methanol–water soluble wheat straw organosolv lignin
NMR	Nuclear magnetic resonance
OSL	Organosolv lignin
PDA	Polydiode array
SKL	Softwood kraft lignin
WS	Wheat straw
WSOSL	Wheat straw organosolv lignin

Data availability

The data supporting this article have been included as part of the ESI.†

Author contributions

REM: investigation, writing – original draft preparation; FF: data curation, writing – original draft preparation; MO: funding, writing – reviewing and editing; CC:

funding, writing – reviewing and editing; HL: conceptualization, methodology, data curation, supervision, writing – reviewing and editing.

Conflicts of interest

There are no conflicts to declare.

Acknowledgements

This work was in part supported by the National Recovery and Resilience Plan (NRRP), Mission 4 Component 2 Investment 1.4 – Call for tender No. 3138 of 16 December 2021, rectified by Decree n.3175 of 18 December 2021 of Italian Ministry of University and Research funded by the European Union – Next Generation EU; Award Number: Project code CN_00000033, Concession Decree No. 1034 of 17 June 2022 adopted by the Italian Ministry of University and Research, CUP H43C22000530001, Project title "National Biodiversity Future Center – NBFC". REM would like to thank the Ministry of Science, Research and Technology of Iran for financial support. All authors would like to thank Compagnie Industrielle de la Matière Végétale (CIMV) (Levallois Perret, France) for providing wheat straw Biolignin™, and Stora Enso (Sunila Mill, Kotka, Finland) for providing Lignoboost softwood kraft lignin.

References

1 *Wood: Chemistry, Ultrastructure, Reactions*, ed. D. Fengel and G. Wegener, De Gruyter, Berlin, New York, 1983.
2 *Lignin Valorization: Emerging Approaches*, ed. G. T. Beckham, Royal Society of Chemistry, Cambridge, 2018.
3 K. Forss and K.-E. Fremer, in *Lignin: Historical, Biological, and Materials Perspectives*, ed. W. G. Glasser, R. A. Northey and T. P. Schultz, American Chemical Society, Washington, DC, 1999, vol. 742, pp. 100–116.
4 *Lignin: Historical, Biological, and Materials Perspectives*, ed. W. G. Glasser, R. A. Northey and T. P. Schultz, American Chemical Society, Washington, DC, 1999, vol. 742.
5 M. Aresta, A. Dibenedetto and F. Dumeignil, *Biorefineries, an Introduction*, De Gruyter, Berlin, Boston, 2015.
6 Z.-H. Liu, H. Liu, T. Xu, Z.-M. Zhao, A. J. Ragauskas, B.-Z. Li, J. S. Yuan and Y.-J. Yuan, *Renewable Sustainable Energy Rev.*, 2025, **211**, 115296.
7 P. Bajpai, in *Carbon Fibre from Lignin*, Springer, Singapore, 2017, pp. 29–32.
8 J. D. Gargulak and S. E. Lebo, in *Lignin: Historical, Biological, and Materials Perspectives*, ed. W. G. Glasser, R. A. Northey and T. P. Schultz, American Chemical Society, Washington, DC, 1999, vol. 742, pp. 304–320.
9 T. Q. Hu, *Chemical Modification, Properties, and Usage of Lignin*, Kluver Academic/plenum Publishers, New York, 2002.
10 S. Sethupathy, G. Murillo Morales, L. Gao, H. Wang, B. Yang, J. Jiang, J. Sun and D. Zhu, *Bioresour. Technol.*, 2022, **347**, 126696.
11 S. Liu, Y. Zhu, Y. Liao, H. Wang, Q. Liu, L. Ma and C. Wang, *Appl. Energy Combust. Sci.*, 2022, **10**, 100062.

12 P. P. Thoresen, H. Lange, U. Rova, P. Christakopoulos and L. Matsakas, *Int. J. Biol. Macromol.*, 2023, **233**, 123471.
13 I. van Zandvoort, E. J. Koers, M. Weingarth, P. C. A. Bruijnincx, M. Baldus and B. M. Weckhuysen, *Green Chem.*, 2015, **17**, 4383–4392.
14 Y. Zhao, U. Shakeel, M. Saif Ur Rehman, H. Li, X. Xu and J. Xu, *J. Cleaner Prod.*, 2020, **253**, 120076.
15 T.-Q. Yuan, S.-N. Sun, F. Xu and R.-C. Sun, *J. Agric. Food Chem.*, 2011, **59**, 10604–10614.
16 X. Du, G. Gellerstedt and J. Li, *Plant J.*, 2013, **74**, 328–338.
17 M. Pan, X. Gan, C. Mei and Y. Liang, *J. Mol. Struct.*, 2017, **1127**, 575–582.
18 M. Andlar, T. Rezić, N. Marđetko, D. Kracher, R. Ludwig and B. Šantek, *Eng. Life Sci.*, 2018, **18**, 768–778.
19 J. Dai, A. F. Patti and K. Saito, *Tetrahedron Lett.*, 2016, **57**, 4945–4951.
20 R. Ma, M. Guo and X. Zhang, *Catal. Today*, 2018, **302**, 50–60.
21 R. Rinaldi, R. Jastrzebski, M. T. Clough, J. Ralph, M. Kennema, P. C. A. Bruijnincx and B. M. Weckhuysen, *Angew. Chem., Int. Ed.*, 2016, **55**, 8164–8215.
22 J. S. Rodrigues, V. Lima, L. C. P. Araújo and V. R. Botaro, *Ind. Eng. Chem. Res.*, 2021, **60**, 10863–10881.
23 T. Pang, G. Wang, H. Sun, W. Sui and C. Si, *Ind. Crops Prod.*, 2021, **165**, 113442.
24 M. Gigli and C. Crestini, *Green Chem.*, 2020, **22**, 4722–4746.
25 R. J. Antonius Gosselink, J. C. van der Putten and D. Stephan van Es, Stichting Dienst Landbouwkundig Onderzoek, WO2015178771(A1), 2015.
26 C. G. Boeriu, F. I. Fițigău, R. J. A. Gosselink, A. E. Frissen, J. Stoutjesdijk and F. Peter, *Ind. Crops Prod.*, 2014, **62**, 481–490.
27 K. Lundquist and T. K. Kirk, *Tappi J.*, 1980, **63**, 80–82.
28 C. Schuerch, *J. Am. Chem. Soc.*, 1952, **74**, 5061–5067.
29 M. Gigli and C. Crestini, *Green Chem.*, 2020, **22**, 4722–4746.
30 H. Sadeghifar and A. Ragauskas, *ACS Sustain. Chem. Eng.*, 2020, **8**, 8086–8101.
31 C. Cui, R. Sun and D. S. Argyropoulos, *ACS Sustain. Chem. Eng.*, 2014, **2**, 959–968.
32 H. Lange, P. Schiffels, M. Sette, O. Sevastyanova and C. Crestini, *ACS Sustain. Chem. Eng.*, 2016, **4**, 5136–5151.
33 T. V. Lourençon, F. A. Hansel, T. A. da Silva, L. P. Ramos, G. I. B. de Muniz and W. L. E. Magalhães, *Sep. Purif. Technol.*, 2015, **154**, 82–88.
34 T. Saito, J. H. Perkins, F. Vautard, H. M. Meyer, J. M. Messman, B. Tolnai and A. K. Naskar, *ChemSusChem*, 2014, **7**, 221–228.
35 V. Passoni, C. Scarica, M. Levi, S. Turri and G. Griffini, *ACS Sustain. Chem. Eng.*, 2016, **4**, 2232–2242.
36 J. A. Hemmingson, *J. Wood Chem. Technol.*, 1987, **7**, 527–553.
37 A. Duval, F. Vilaplana, C. Crestini and M. Lawoko, *Holzforschung*, 2015, **70**, 11–20.
38 J.-Y. Kim, S. Young Park, J. Hoon Lee, I.-G. Choi and J. Weon Choi, *RSC Adv.*, 2017, **7**, 53117–53125.
39 R. Ebrahimi Majdar, A. Ghasemian, H. Resalati, A. Saraeian, C. Crestini and H. Lange, *Polymers*, 2019, **11**, 225.
40 R. E. Majdar, C. Crestini and H. Lange, *ChemSusChem*, 2020, **13**, 4735–4742.

41 O. Sevastyanova, M. Helander, S. Chowdhury, H. Lange, H. Wedin, L. Zhang, M. Ek, J. F. Kadla, C. Crestini and M. E. Lindström, *J. Appl. Polym. Sci.*, 2014, **131**, 40799.
42 A. Duval, S. Molina-Boisseau and C. Chirat, *Holzforschung*, 2014, **69**, 127–134.
43 L. Dai, W. Zhu, J. Lu, F. Kong, C. Si and Y. Ni, *Green Chem.*, 2019, **21**, 5222–5230.
44 R. Ebrahimi Majdar, A. Ghasemian, H. Resalati, A. Saraeian, C. Crestini and H. Lange, *ACS Sustain. Chem. Eng.*, 2020, **8**, 16803–16813.
45 P. Tomani, *Cellul. Chem. Technol.*, 2010, **44**, 53–58.
46 M. Delmas and B. B. Mlayah, Compagnie Industrielle de la Matiére Végétale - CIMV, WO2011154293(A1), 2011.
47 N. Tachon, B. Benjelloun-Mlayah and M. Delmas, *BioResources*, 2016, **11**, 5797–5815.
48 L. Mbotchak, C. Le Morvan, K. L. Duong, B. Rousseau, M. Tessier and A. Fradet, *J. Agric. Food Chem.*, 2015, **63**, 5178–5188.
49 N. Cachet, S. Camy, B. Benjelloun-Mlayah, J.-S. Condoret and M. Delmas, *Ind. Crops Prod.*, 2014, **58**, 287–297.
50 J. Snelders, E. Dornez, B. Benjelloun-Mlayah, W. J. J. Huijgen, P. J. de Wild, R. J. A. Gosselink, J. Gerritsma and C. M. Courtin, *Bioresour. Technol.*, 2014, **156**, 275–282.
51 G.-H. Delmas, B. Benjelloun-Mlayah, Y. L. Bigot and M. Delmas, *J. Appl. Polym. Sci.*, 2011, **121**, 491–501.
52 C. Crestini, H. Lange, M. Sette and D. S. Argyropoulos, *Green Chem.*, 2017, **19**, 4104–4121.
53 C. M. Hansen, *Hansen Solubility Parameters: A User's Handbook, Second Edition*, CRC Press, 2007.
54 A. Granata and D. S. Argyropoulos, *J. Agric. Food Chem.*, 1995, **43**, 1538–1544.
55 X. Meng, C. Crestini, H. Ben, N. Hao, Y. Pu, A. J. Ragauskas and D. S. Argyropoulos, *Nat. Protoc.*, 2019, **14**, 2627–2647.
56 H. Lange, F. Rulli and C. Crestini, *ACS Sustain. Chem. Eng.*, 2016, **4**, 5167–5180.
57 F. Lu and J. Ralph, *J. Agric. Food Chem.*, 1997, **45**, 4655–4660.
58 P. Paulsen Thoresen, H. Lange, U. Rova, P. Christakopoulos and L. Matsakas, *Bioresour. Technol.*, 2023, **369**, 128447.
59 H. Sotome-Yukisada, K. Hiratsuka, K. Noguchi, J. Ashida, T. Kato, K. Shikinaka, Y. Matsushita, Y. Otsuka and Y. Tominaga, *Anal. Chem.*, 2025, **97**, 9512–9517.
60 D. F. Cipriano, L. S. Chinelatto, S. A. Nascimento, C. A. Rezende, S. M. C. de Menezes and J. C. C. Freitas, *Biomass Bioenergy*, 2020, **142**, 105792.

